THE ASTROPHYSICAL JOURNAL, 251:L109–L114, 1981 December 15

A NEW COMPONENT OF HARD X-RAYS IN SOLAR FLARES

R. P. LIN AND R. A. SCHWARTZ
Space Sciences Laboratory, University of California, Berkeley
R. M. PELLING
Center for Astrophysics and Space Science, University of California at San Diego
AND
K. C. HURLEY
Centre d'Etude Spatiale des Rayonnements, Toulouse, France
Received 1981 June 1; accepted 1981 September 2

ABSTRACT

We present high resolution (~ 1 keV FWHM) spectral measurements from 13 to 300 keV of a solar flare hard X-ray burst observed on 1980 June 27 by a balloon-borne array of cooled germanium planar detectors. At energies below ~ 35 keV we identify a new component of solar flare hard X-rays. This component is characterized by an extremely steep spectrum which fits closely to that from a Maxwellian electron distribution with a maximum temperature of $\sim 34 \times 10^6$ K and an emission measure of 2.9×10^{48} cm^{-3}. This hot isothermal component appears at the peak of the normal power-law-like impulsive X-ray burst component, and it remains isothermal and dominates the X-ray emission below ~ 30 keV through the decay of the flare event.

Subject headings: Sun: flares — Sun: X-rays

I. INTRODUCTION

X-ray, radio, and energetic particle measurements have shown that the acceleration of ~ 10–10^2 keV electrons commonly occurs during the flash phase of solar flares (see review by Lin 1974). Most of our quantitative information about flare-accelerated electrons at the Sun comes from hard, $\gtrsim 20$ keV X-ray observations. Usually the $\gtrsim 20$ keV X-ray burst observed during the impulsive phase is assumed to be a single component. The observations are generally consistent with a falling power-law spectrum, with some evidence for a change to a more rapidly decreasing spectrum above an energy of 60–100 keV (Kane and Anderson 1970), although some flare bursts have been reported to be consistent with an isothermal source spectrum with temperatures of 10^8–10^9 K (Crannell *et al.* 1978; Elcan 1978). The broad energy channel data available from scintillation detectors, however, appear inadequate to distinguish between power-law and isothermal spectra (see review by Kane *et al.* 1980).

Accurate measurements of the hard X-ray spectrum are important for studying the flare energy release process. If the observed X-ray emission is produced by bremsstrahlung from fast electrons colliding with a cold plasma (i.e., fast electron energy $\gg kT$), then the Coulomb collision energy losses would be 10^4–10^5 times the X-ray losses. Under this nonthermal assumption, a large fraction of the total flare energy in many flares must be initially contained in the fast electrons (Lin and Hudson 1971, 1976); the exact amount depends on how low in energy the fast electron spectrum extends. The electron acceleration process would then be intimately related to the flare energy release process. Under alternative, thermal interpretations, the hard X-ray emission is produced by a very hot, $T \approx 10^8$–10^9 K, plasma (Chubb 1970; Brown 1975; Kahler 1975). Then electron-electron Coulomb collisions will result in exchanges of energy only among the hot electrons without any net collisional energy loss. Provided the hot plasma could be confined, the energy requirements for the energetic electrons might be drastically reduced (see discussion in Ramaty *et al.* 1980). In the case of a homogeneous source (e.g., the adiabatic heating model of Mätzler *et al.* [1978] or the high density, thermonuclear burning model of Colgate, Audouze, and Fowler [1977]), a Maxwellian electron distribution would be expected.

In this *Letter* we describe the characteristics of a previously unidentified component in the hard X-ray range, which is observed to occur starting at the maximum of the normal impulsive hard X-ray component. This new component has an extremely steep X-ray spectrum characteristic of an isothermal plasma with temperatures of ~ 30–35×10^6 K and an emission measure of a few times 10^{48} cm^{-3}.

II. EXPERIMENTAL DETAILS

The observations were made with two coaligned hard X-ray detector systems: an array of four planar intrinsic

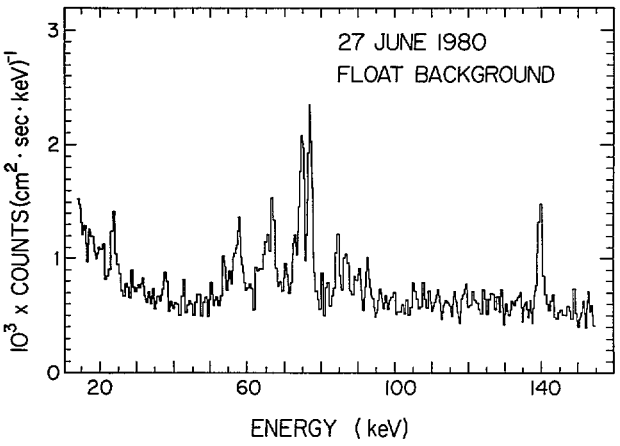

FIG. 1.—Energy spectrum of the detector background at balloon float altitude, all four detectors summed together. The two largest peaks are separated by ~ 2 keV.

germanium detectors, each 4 cm diameter by 1.3 cm thick, cooled by liquid nitrogen to obtain $\lesssim 1$ keV FWHM energy resolution; and a 300 cm^2 NaI/CsI phoswich scintillator for high time resolution (Peterson 1975). The cryostat housing the germanium detector array is surrounded by a ~ 2″ thick CsI anticoincidence well. Graded Z passive collimators provide 2°.6 × 5°.2 fields of view for both detector systems. Each Ge detector output goes to a pulsed FET feedback preamplifier, dual fast (400 ns) and slow (~ 10 μs) shaping amplifiers, and then to a 4096 channel ADC covering the interval ~ 11–580 keV (7 bins per keV). The fast amplifier provides for coincidence and pile-up rejection so that rates up to ~ 20,000 counts s^{-1}, far greater than those observed during the flare, can be handled without spectral distortion (Landis, Goulding, and Pehl, 1971). Figure 1, a background energy spectrum at balloon float altitude with all four detector outputs summed together, shows the excellent energy resolution ($\lesssim 1$ keV). This resolution is the best ever achieved in an instrument flown for astrophysical measurements from ~ 15 to ~ 200 keV. An on-board flare burst memory provides high time resolution accumulations (to 8 ms) for the two-detector system in four energy channels.

The instrument was flown from Palestine, Texas, on 1980 June 27. Observations of the Sun and the Crab Nebula were taken beginning at float at 1520 UT until 2130 UT. During the solar X-ray burst of interest, the balloon was at an atmospheric depth of 2.3 g cm^{-2}, as determined by an on-board pressure sensor accurate to ±2%. This gave a line-of-sight atmospheric depth to the Sun of 2.73 g cm^{-2}. Tracking was achieved with an alt-azimuth pointing system on the gondola with 1 minute pointing updates. During solar observation an optical sensor provided azimuthal reference.

Each Ge detector count rate was normalized for detector live time, and the nonflare background was subtracted. The high energy resolution and narrow field of view of the germanium detector system permit very accurate source spectra to be obtained with a relatively simple spectral unfolding procedure. This procedure takes into account collimator transmission; detector efficiency (including fluorescent escape and Compton effects); and attenuation by the Be window, thermal insulation, and the overlying atmosphere.

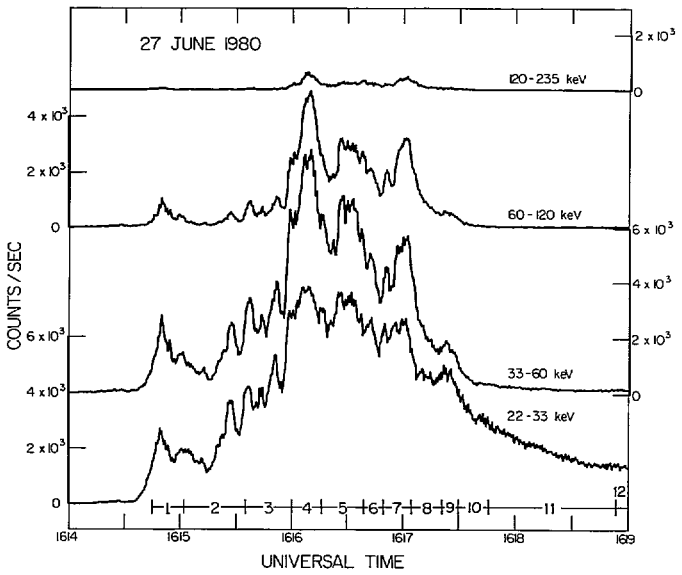

FIG. 2.—The flare hard X-ray burst observed by the scintillation detector. The numbered intervals at the bottom indicate the times when spectra were accumulated for the germanium detector array.

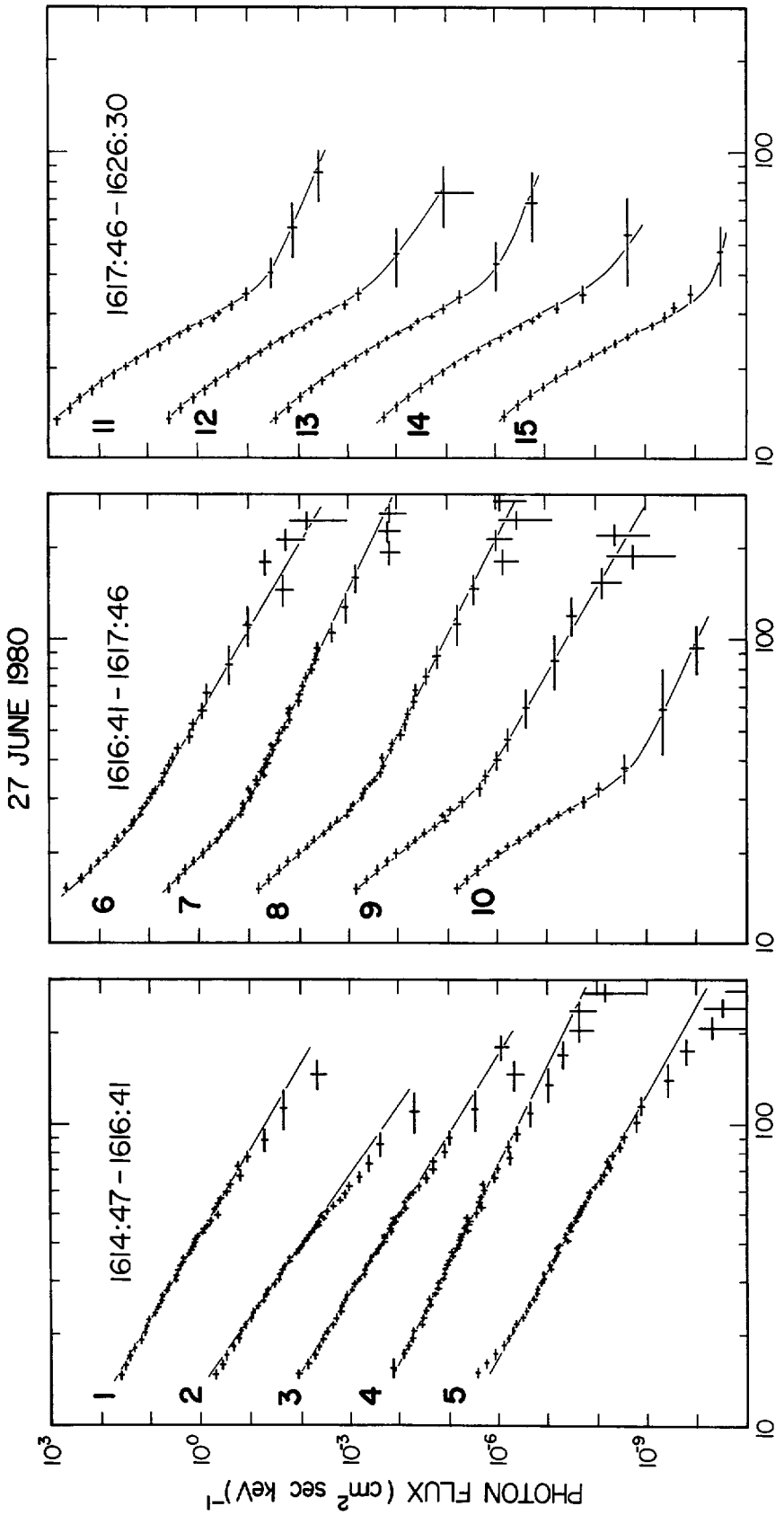

FIG. 3.—Energy spectra from the germanium array through the event. The vertical scale applies to the uppermost spectrum, with each succeeding spectrum offset downward by two decades.

III. RESULTS

The hard X-ray event (Fig. 2) consists of a series of impulsive bursts, each of duration of a few to a few tens of seconds, beginning ~ 1614 UT, reaching an overall peak at ~ 1616:10, and ending ~ 1617:30, followed by a long slow decay (visible in the 22–33 keV channel) which lasts till ~ 1632 UT. The associated Hα flare began at 1615 UT and peaked at 1617 UT. It was located at S27, W67 in plage region No. 2522 and reported to be only of importance SB. Intense microwave emission (325 sfu at 2800 MHz), a group of strong type III–V bursts, and type II and IV emission, however, were observed to accompany the flare. The *Solar Maximum Mission* (*SMM*) coronagraph observed a coronal transient about 20 minutes later (W. Wagner, private communication). Unfortunately, the flare itself was during *SMM* nighttime. An M6 soft X-ray burst was observed by the *GOES 2* spacecraft, and the hard X-ray burst was also observed by the *ISEE 3* spacecraft (S. R. Kane, private communication).

We have used ratios of adjacent energy channels of the scintillator to choose time intervals (indicated in Fig. 2) over which the energy spectrum is relatively constant. Accurate energy spectra were then determined for these intervals from the germanium spectrometer in 8 channel wide (1.12 keV) bins. Adjacent bins were summed together if required for good statistical accuracy. The resulting spectra are shown in Figure 3. At the start of the event, the spectra are accurately power law (index ~ 3.5) from 13 keV up to ~ 60–100 keV, with a steepening at higher energies. Detailed analysis of this "normal" power-law component will be presented in a future paper, but we note here that single temperature isothermal fits to this component clearly can be excluded by using χ^2 tests. Note also that this power-law component persists to the end of the event, well after the impulsive phase.

Beginning near the peak of the event at ~ 1616 UT, a new, very steep component is observed at low energies, superposed on the power law. At its steepest, this new component has a power-law index $\gamma \sim 11$, where $(dJ/dE) \propto E^{-\gamma}$. Such a steep spectrum is unresolvable by scintillation detectors. This steep component appears to vary much more slowly than the power-law component. After the rapid drop of the power-law component at ~ 1617 UT, it can be seen that the new steep component has a curved exponential-like spectral shape. We have fit the X-ray spectrum to a combination of that expected from a single temperature Maxwellian electron distribution,

$$\frac{dn_e}{dE_e} = 2\pi n_e \left(\frac{1}{\pi kT}\right)^{3/2} E_e^{1/2} e^{-E_e/kT}$$

at low energies, and a power law at high energies. Here n_e, m_e, and E_e refer to the electron number density, mass, and energy, respectively. The power-law component contributes insignificantly to the flux below ~ 30 keV. The X-ray spectrum from this distribution was computed for solar coronal abundances ($\bar{Z}^2 = 1.8$) using the Bethe-Heitler bremsstrahlung cross sections with the Elwert correction (Koch and Motz 1959). These are estimated to be accurate to 10% in the 10–100 keV region.

Figure 4 shows the detailed fit for one of the time intervals. We have estimated the significance of the isothermal fit to the data below 33.5 keV, using the parameter estimation technique of Lampton, Margon, and Bowyer (1976). The 90% confidence (χ^2 fit with 16 degrees of freedom) region in the temperature/emission

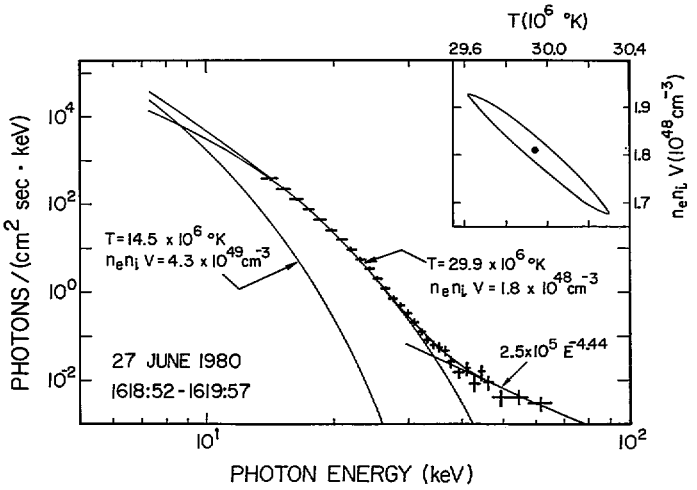

FIG. 4.—Example of the isothermal fit. The power-law fit at high energies and the emission from the flare plasma at low energies are also shown. The χ^2 90% confidence contour is shown in the upper right corner.

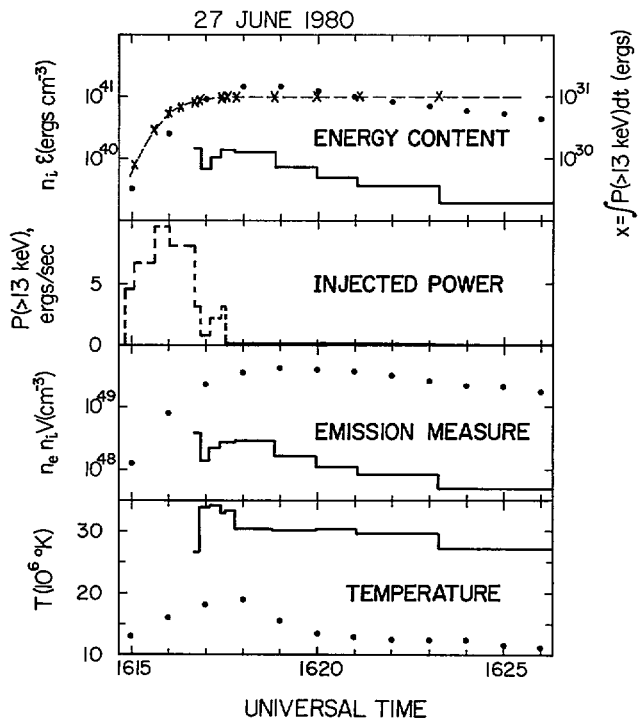

FIG. 5.—The evolution in time of the parameters of the hot isothermal component (*solid lines*) and the flare plasma (*dots*). The energy input rate and cumulative total energy of the power-law component are shown (*x's and dashed lines*) also.

measure plane is also shown in Figure 4. The best-fit temperature is 29.9×10^6 K, and the emission measure is 1.8×10^{48} cm^{-3}. Good fits to isothermals are obtained throughout the decay phase (> 1618 UT) of the event. Thus this X-ray component is consistent with that of an isothermal electron distribution essentially throughout its existence. The evolution of the temperature and emission measure with time for this component is shown in Figure 5 (solid lines). The maximum temperature of 34.2×10^6 K is reach at ~ 1617:15 UT, and the maximum emission measure of 2.9×10^{48} cm^{-3} is attained at ~ 1618 UT (excluding the value before ~ 1616:40 UT which is highly uncertain because the power-law component dominates).

IV. DISCUSSION

To investigate the relationship of this hot isothermal component to the soft X-ray producing thermal flare plasma which has been studied previously (Moore *et al.* 1980), we have used 1–8 Å and 0.5–4 Å ionization chamber data from the *GOES 2* spacecraft (R. Donnelly, private communication). These data were fit to a single temperature and emission measure using the *GOES 2* chambers' response functions (Donnelly, Grubb, and Cowley 1977) and the calculated X-ray emission as a function of temperature for an isothermal coronal gas (Wendt, private communication; Mewe 972; Tucker and Koren 1971). The maximum temperature reached by the flare plasma is 19×10^6 K, well below that of the hot isothermal component, and the maximum emission measure is 4×10^{49} cm^{-3}, a factor of 14 larger. In our energy range (> 13 keV) the X-ray emission of this flare plasma would be negligible compared to the observed X-ray flux (Fig. 4). Since the flare plasma usually consists of a continuous distribution of emission measures with temperature (Moore *et al.* 1980), the hot isothermal component identified here could be the highest temperature portion of this distribution. In that case, these observations show that the flare plasma at least occasionally extends up to 35×10^6 K. Both the emission measure and temperature of the hot isothermal component, however, show temporal variations quite different from those of the flare plasma (Fig. 5). Note especially the rapid rise in temperature at 1616:50 UT and rapid fall at 1617:45 UT for the hot isothermal component, quite independent of the slow smooth increase in temperature of the flare plasma from 1615 to 1618 UT.

The energy content in the electron plasma, $Q = 3/2 n_e kT$, multiplied by the ambient density, n_i, for both the hot isothermal and the flare plasmas is shown in Figure 5, along with the energy deposition rate (ergs s^{-1}) and the cumulative energy deposited (ergs) for the power-law component, calculated under the thick target assumption. (i.e., that the electrons lose all their

energy by Coulomb collisions). The low energy cutoff is chosen to be 13 keV, since the power-law spectrum is observed to extend down to that energy early in the event. If we assume a maximum source size of 10^5 km (10^{30} cm^3 volume) for the hot isothermal component, then we obtain a lower limit of $\sim 10^9$ cm^{-3} to the ambient density, n_i. Assuming that the observed energy loss for this component is entirely due to radiation gives an upper limit of order $n_i \sim 10^{12}$ cm^{-3}. The total energy contained in this hot isothermal component thus ranges from 10^{28}–10^{31} ergs at maximum, compared to 10^{30}–10^{31} ergs for the thermal flare plasma (for $n_i \sim 10^{10}$–10^{11} cm^{-3}), and a cumulative, thick target energy deposited in the power-law component of $\gtrsim 10^{31}$ ergs. The temporal evolution of the quantities shown in Figure 5 is consistent with the power-law component being the source of energy both for the flare plasma, for typical values of the density, $n_i \sim 10^{10}$–10^{11} cm^{-3} (Moore *et al.* 1980; Widing and Dere 1977), and for the hot isothermal plasma.

We believe that this hot isothermal component may occur commonly in flares, often showing up as a slow decay in the lowest energy channel (typically $\sim$ 20–25 keV) in hard X-ray bursts observed by scintillation detectors. Since at energies below $\sim$ 30 keV this component is significant beginning at the peak of the hard X-ray burst, spectral measurements by scintillation detectors of the power-law component could be substantially distorted. Clearly, high energy resolution is required for unambiguous spectral measurements of the power-law component as well as this hot isothermal component.

We thank J. H. Primbsch, R. Pehl, D. Malone, and F. Duttweiler for their efforts in the development, fabrication, and flight of this instrument. G. Jung helped with the analysis of the data. K. A. Anderson, J. Matteson, and L. Peterson were involved in the planning for this instrument. Discussions with G. Hurford, H. S. Hudson, and S. R. Kane were useful in the interpretation of the data. D. Atkinson and W. Mote assisted with flight preparations as part of the University of California Research Expeditions Program. The research at UCB was supported by NASA grants NSG 7527, NSG 7592, and NGL 05-003-017; and NSF grant ATM 79-24559. The research at UCSD was supported by NASA grant NGL 05-005-003.

REFERENCES

Brown, J. C. 1975, *Solar Gamma-, X-, and EUV-Radiation*, ed. S. R. Kane (Dordrecht: Reidel), p. 245.
Chubb, T. A. 1970, *Proc. Leningrad Symposium, Solar Terrestrial Physic/1970, part I*, ed. E. R. Dyer (Dordrecht: Reidel), p. 99.
Colgate, S. A., Audouze, J., and Fowler, W. A. 1977, *Ap. J.*, **213**, 849.
Crannell, C. J., Frost, K. J., Mätzler, C., Ohki, K., and Saba, J. L., 1978, *Ap. J.*, **223**, 620.
Donnelly, R. F., Grubb, R. N. and Cowley, F. C. 1977, *NOAA Technical Memorandum* (ERL SEL-48).
Elcan M. J. 1978, *Ap. J. (Letters)*, **226**, L99.
Kahler, S. 1975, *Solar Gamma-, X-, and EUV-Radiation*, ed. S. R. Kane (Dordrecht: Reidel), p. 211.
Kane, S. R., and Anderson, K. A. 1970, *Ap. J.*, **162**, 1002.
Kane, S. R. *et al.* 1980, *Solar Flares*, ed. Peter A. Sturrock (Boulder: Colorado Associated University Press), p. 187.
Koch, H. W., and Motz, J. W. 1959, *Rev. Mod. Phys.*, **31**, 920.
Lampton, M., Margon, B. and Bowyer, S. 1976, *Ap. J.*, **208**, 177.
Landis, D. A., Goulding, F. S., and Pehl, R. H. 1971, *IEEE Trans. Nucl. Sci.*, **NS-18**, No. 1, Part I, 115.
Lin, R. P. 1974, *Space Sci. Rev.*, **16**, 189.
Lin, R. P., and Hudson, H. S. 1971, *Solar Phys.*, **47**, 412.
_____. 1976, *Solar Phys.*, 50, 153.
Mätzler, C., Bai, T., Crannell, C. J., and Frost, K. J. 1978, *Ap. J.*, **223**, 1058.
Mewe, R. 1972, *Solar Phys.*, **22**, 459.
Moore, R. *et al.* 1980, *Solar Flares*, ed. Peter A. Sturrock (Boulder: Colorado Associated University Press), p. 341.
Peterson, L. E. 1975, *Ann. Rev. Astr. Ap.*, **13**, 423.
Ramaty, R. *et al.* 1980, *Solar Flares*, ed. Peter A. Sturrock (Boulder: Colorado Associated University Press), p. 117.
Tucker, W. H., and Koren, M. 1971, *Ap. J.*, **168**, 283.
Widing, K. G., and Dere, K. P., 1977, *Solar Phys.*, **53**, 431.

K. C. HURLEY: Centre d'Etude Spatiale des Rayonnements, 9, Avenue de Colonel Roche, 31400 Toulouse, France, CNRS-UPS

R. P. LIN and R. A. SCHWARTZ: Space Sciences Laboratory, University of California, Berkeley, CA 94720

R. M. PELLING: Center for Astrophysics and Space Science, University of California at San Diego, La Jolla, CA 92093